NEURODEVELOPMENT

Sensation is dispensable for the maturation of the vestibulo-ocular reflex

Paige Leary[1]*, Celine Bellegarda[1], Cheryl Quainoo[1], Dena Goldblatt[1,2], Başak Rosti[1], David Schoppik[1]*

Vertebrates stabilize gaze using a neural circuit that transforms sensed instability into compensatory counterrotation of the eyes. Sensory feedback tunes this vestibulo-ocular reflex throughout life. We studied the functional development of vestibulo-ocular reflex circuit components in the larval zebrafish, with and without sensation. Blind fish stabilize gaze normally, and neural responses to body tilts mature before behavior. In contrast, synapses between motor neurons and the eye muscles mature with a time course similar to behavioral maturation. Larvae without vestibular sensory experience, but with mature neuromuscular junctions, had a strong vestibulo-ocular reflex. Development of the neuromuscular junction, and not sensory experience, therefore determines the rate of maturation of an ancient behavior.

Early sensory deprivation profoundly disrupts neural function and associated behaviors in visual (*1*), auditory (*2*), and vestibular (*3*, *4*) systems, and sensory feedback is responsible for tuning mature vestibular behaviors (*5*). Sensory experience might therefore set the pace at which neural circuits and the behaviors they subserve emerge; alternatively, such functional maturation might reflect development of the underlying circuit components. Although each component of a neural circuit plays a necessary role in generating behavior, a component's necessity does not confer rate-limiting status. Instead—by analogy to chemistry (*6*)—a rate-limiting component would be one whose development is the most protracted, determining the rate at which behavior can reach maturation. Despite recent technological improvements in connectomics for circuit identification (*7*, *8*), the complexity and in utero development (*9*) of mammalian circuits complicates measuring rates of development and their link to specific behaviors.

We studied an archetypal sensorimotor circuit that stabilizes gaze in a simple model vertebrate, the larval zebrafish. The relative simplicity and high conservation of this circuit across vertebrates (*10*) have made larval zebrafish a powerful model to uncover neural mechanisms of sensorimotor behavior (*11*). The vestibulo-ocular reflex circuit consists of sensory afferents, central interneurons, and motor neurons that together transform head and body tilts into counterrotatory eye movements (*12*) (Fig. 1A). When mature, this feed-forward circuit generates eye movements matching the head and body velocity, minimizing retinal slip and stabilizing gaze. In vertebrates, both gaze stabilization and vestibulo-ocular reflex circuit components mature during early development (*13*). In this study, we used the transparent, externally developing larval zebrafish to determine the role of sensation in vestibulo-ocular reflex circuit development.

Early maturation of gaze stabilization behavior

To determine when behavior matures, we measured the eyes' response to body tilts across early development (Fig. 1B). We previously used this approach to define the frequency response of the vestibulo-ocular reflex (*14*). Briefly, fish were immobilized with their eye freed and tilted in the pitch axis (nose-up or nose-down) on a rotating platform in complete darkness. Tilt magnitude (15°) and peak velocity (35°/s) were selected to match the statistics of pitch tilts observed in freely swimming larvae (*15*). At and after 5 days post-fertilization (dpf), fish rotated their eyes down in response to nose-up pitch tilt stimuli (Fig. 1C). A mature vestibulo-ocular reflex will counterrotate the eyes at the same velocity as the body and head, eliminating residual image motion (retinal slip) and stabilizing gaze. We therefore parameterized behavioral performance as the ratio of the peak eye velocity to the peak platform velocity (gain). A gain of 1 is fully compensatory and mature, 0 indicates that the eye does not move, and gains between 0 and 1 reflect immature and inadequate gaze stabilization. Gain improved with age from 3 to 9 dpf ($P_{ANOVA} = 1.01 \times 10^{-9}$; ANOVA, analysis of variance; Fig. 1D), reached gains of ~1, and did not change between 9 and 15 dpf ($P_{post\ hoc} = 0.95$). These data indicate that behavior improves gradually over the first week of life and performance plateaus at ~9 dpf.

Gaze stabilization develops normally in congenitally blind fish

As the vestibulo-ocular reflex minimizes retinal slip, we first sought to determine how the absence of visual feedback during early life would affect the development of gaze stabilization behavior. Visual feedback is particularly important because fish ocular muscles do not contain proprioceptors (Golgi tendon organs and muscle spindles). We raised congenitally blind fish to ~9 dpf (see methods in the supplementary materials for details) and measured eye rotations in response to body tilts, as in Fig. 1 (fig. S1). Blind fish and sighted siblings showed similar gain ($P_{ANOVA} = 0.934$). Despite its importance for calibrating gain in mature animals, visual information is therefore dispensable for the development of the vestibulo-ocular reflex.

Vestibular neuron responses plateau well before behavioral performance peaks, with or without motor neuron–derived feedback

Given that visual feedback is dispensable, either the slowest component of the circuit to develop and/or nonvisual feedback could constrain behavioral maturation. Vestibular interneurons make up the central node of a feed-forward circuit, where their activity encodes body and head tilt magnitude and direction (Fig. 2A). To measure the development of vestibular responses to body tilts, we recorded neural activity at eccentric body postures (Fig. 2B).

We used Tilt In Place Microscopy (TIPM) (*16*) to avoid rotating the microscope. TIPM returns fish from an eccentric orientation to the imaging plane faster (~5 ms) than the time constant of the calcium indicator (GCaMP6s) (*17*). The activity observed reflects the decay of the neuron's eccentric response upon return to horizontal. Central neurons in the tangential vestibular nucleus that project to extraocular motor nuclei nIII and nIV are indispensable for the vestibulo-ocular reflex (*14*, *18*). They respond exclusively to either nose-up or nose-down tilts (*19*), and, when activated optogenetically, they induce torsional eye rotations (*18*). We performed longitudinal TIPM (±25°) in these neurons to determine when their responses plateau. We found that vestibular neuron response strength increases drastically between 3 and 5 ($P_{t\ test} = 1.2 \times 10^{-3}$, $n = 22$ neurons, $N = 7$ fish) but not between 5 and 7 or 7 and 9 dpf ($P_{t\ test} = 0.067$, $n = 21$ neurons, $N = 7$ fish; Fig. 2, C to E). Although both behavior and vestibular neuron responses improved between 4 and 5 dpf, vestibular neuron response strength reached a plateau well before behavioral performance is mature. The slowest component to mature must therefore be downstream of central vestibular interneurons.

To determine whether motor-derived feedback influences the maturation of vestibular neuron responses, we adopted a loss-of-function approach. We performed TIPM to measure vestibular neuron responses on a *phox2a* mutant background (*20*) that fails to develop nIII and nIV extraocular motor neurons (Fig. 2, A, F,

[1]Department of Otolaryngology, Department of Neuroscience and Physiology, and the Neuroscience Institute, NYU Grossman School of Medicine, New York, NY, USA. [2]Center for Neural Science, New York University, New York, NY, USA.
*Corresponding author. Email: paigebelleleary@gmail.com (P.L.); schoppik@gmail.com (D.S.)

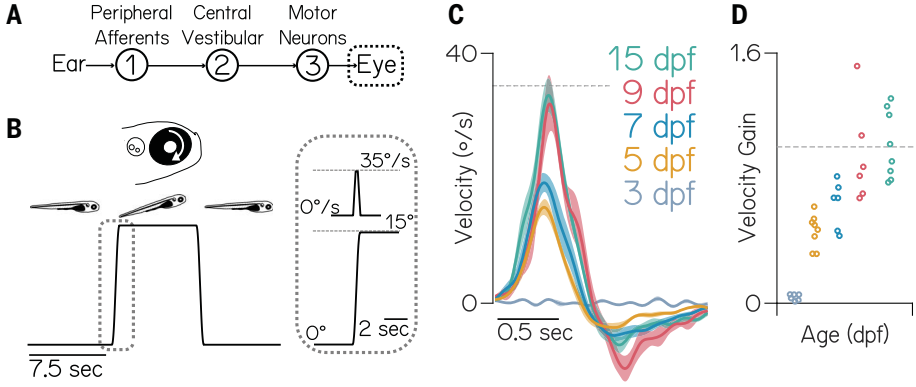

Fig. 1. Gaze stabilization matures by 9 days postfertilization. (**A**) Diagram of the feed-forward gaze stabilization circuit. Tilts are sensed by the utricle in the inner ear; information then flows through the eighth cranial nerve peripheral afferents (1) to central vestibular neurons in the brainstem (2) to motor neurons in cranial nuclei nIII and nIV (3) that counterrotate the eye. (**B**) Schematic of body tilt stimulus. Gray dotted box shows the trapezoidal velocity profile and angle of the tilt. (**C**) Average eye velocity ± SEM at 3, 5, 7, 9, and 15 dpf (N = 6, 8, 6, 6, and 8 fish). Gray line at the peak tilt velocity (35°/s). (**D**) Gain (peak eye velocity divided by peak table velocity) for each fish (peak table velocity = 35°/s); color indicates age as in (C). Three versus 5 dpf gains, $P_{post\ hoc}$ = 0.0021; 3 versus 7 dpf gains, $P_{post\ hoc}$ = 6.51 × 10^{-5}; 3 versus 9 dpf gains, $P_{post\ hoc}$ = 4.57 × 10^{-8}; 9 versus 15 dpf gains, $P_{post\ hoc}$ = 0.95. Horizontal line at gain = 1.

and G). After ±19° tilts, responses of individual vestibular neurons (Fig. 2H) increased between 3 and 5 dpf for both sibling fish and mutants (P_{ANOVA} = 1.95 × 10^{-26}, age × genotype P_{ANOVA} = 0.053; 3 dpf: n = 137 neurons over N = 5 siblings, n = 88 neurons/N = 5 mutants; 5 dpf: n = 113 neurons/N = 5 siblings, n = 116 neurons/N = 5 mutants). Across fish (Fig. 2I), the average response of paired (tracked) neurons increased between 3 and 5 dpf (P_{ANOVA} < 10 × 10^{-16}) with no effect of genotype (P_{ANOVA} = 0.069). Finally, to evaluate the development of peripheral vestibular inputs, we examined directional selectivity at 5 dpf. Consistent with a previous report (*19*), the ratio of nose-up and nose-down sensitive (directionality index values < |0.1|) neurons was nearly even, with no difference between genotype ($P_{K\text{-}S\ test}$ = 0.66; 51.9 ± 6% nose-up, 48 ± 6% nose-down, n = 118 neurons over N = 5 siblings; 48.1 ± 13% nose-up stimuli, 51.8 ± 13% nose-down, n = 117/N = 5 *phox2a* mutants) (Fig. 2J). These results establish that, even without motor neurons—and, by extension, motor-derived

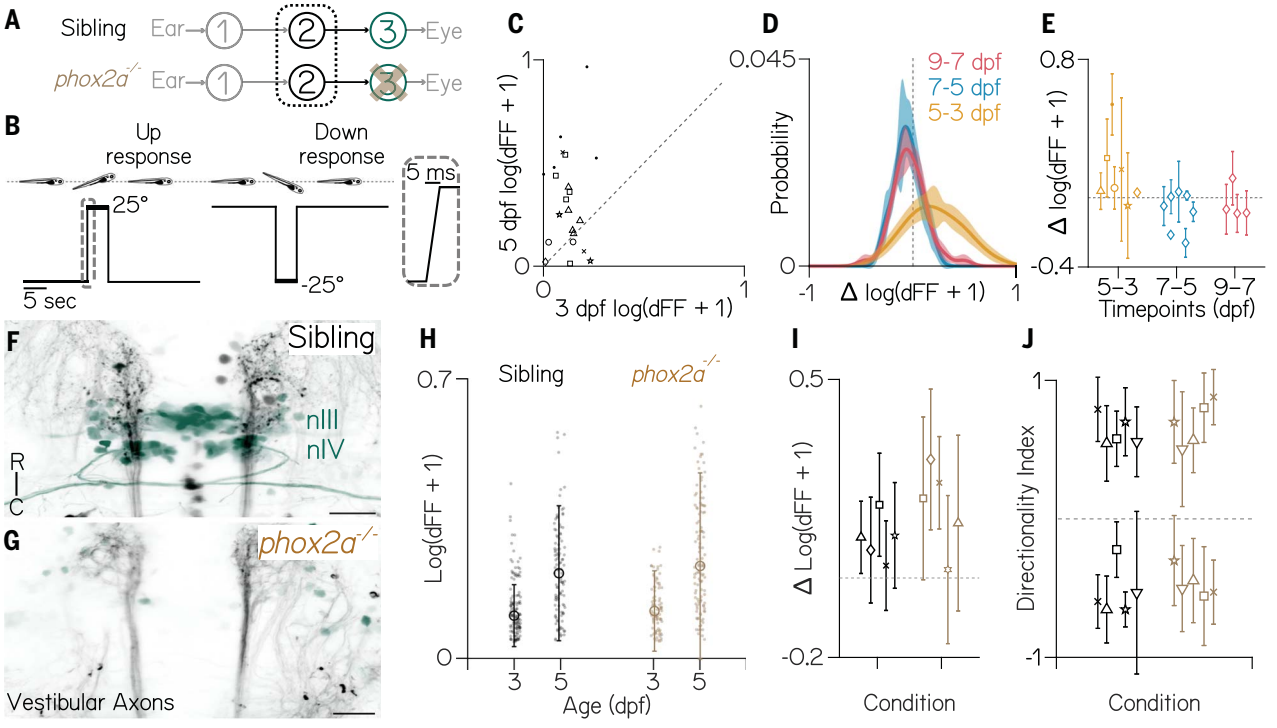

Fig. 2. Central vestibular neuron responses plateau between 3 and 5 dpf, with or without motor neurons. (**A**) Diagram of the gaze stabilization circuit, focused on vestibular neurons in fish with (green) and without (brown, *phox2a*) motor neurons in cranial nuclei nIII and nIV. (**B**) A pitch-tilt stimulus trial with a 15-s baseline, a rapid step (inset, 25° step), a 5-s eccentric hold, and a rapid return for imaging. (**C**) Comparison of neural responses (the change in fluorescence divided by basal fluorescence, or dFF) to 25° nose-up steps at 3 and 5 dpf ($P_{t\ test}$ = 1.2 × 10^{-3}). Dashed line at 0. (**D**) Distribution ± bootstrapped SD of pairwise differences of individual neurons between days (5 and 3, 7 and 5, and 9 and 7 dpf) in response to 25° steps. (**E**) Data from (D), plotted as the median pairwise difference ± interquartile ratio (IQR) for neurons from each individual fish (N = 7, 7, and 4). Five to 7 versus 7 to 9 dpf ($P_{t\ test}$ = 0.067 and 0.22, respectively). Dashed line at 0. (**F** and **G**) Axons of central vestibular nuclei (black) to motor neurons in nIII and nIV (green) in a 3 dpf sibling and *phox2a* mutant. Scale bars: 25 μm. R, rostral; C, caudal. (**H**) Individual neuron responses (dots) to 19° pitch tilts in their preferred direction at 3 and 5 dpf in *phox2a*$^{-/-}$ mutants and controls (P_{ANOVA} for response change over time < 10 × 10^{-16}; P_{ANOVA} for age and genotype interactions < 10 × 10^{-16}). Median ± IQR overlaid. (**I**) Data from (H), plotted as the median pairwise difference ± IQR for paired neurons from each individual fish (n = 113 neurons/N = 5 siblings, n = 116/N = 5 *phox2a* mutants; P_{ANOVA} = 5.03 × 10^{-9} for age effect, P_{ANOVA} = 0.068 for interactions of age and genotype). Dashed line at 0. (**J**) Directionality indices of vestibular neurons in *phox2a*$^{-/-}$ mutants (N = 5 fish, n = 102 neurons) and controls (N = 5, n = 112), plotted as the median ± IQR for each fish ($P_{K\text{-}S\ test}$ = 0.66).

feedback—vestibular neuron responses develop early relative to behavior.

Extraocular motor neuron responses develop between 3 and 5 dpf

As the last central node in a feed-forward reflex, extraocular motor neuron activity reflects all sensory inputs from the entire circuit (Fig. 3A). Consequentially, if the development of motor neuron responses reaches a plateau earlier than behavioral improvement, the slowest developmental process must be in the motor periphery. We repeated longitudinal TIPM (±25°) to determine when motor neuron responses plateau. However, as the calcium responses of motor neurons have not been evaluated in response to body tilts, we first characterized the tuning and sensitivity properties of these neurons to a gradient of stimulus steps (Fig. 3B). To match the pulling direction of the muscle, superior oblique motor neurons should respond predominantly to nose-up tilts. As expected, superior oblique neurons at 5 dpf responded unidirectionally to nose-up body tilts (Fig. 3C) but not to nose-down body tilts (Fig. 3D). Motor neuron activity at 5 dpf varied as a function of nose-up tilt eccentricity (n = 22/32 neurons with slope > 0, $P_{\text{post hoc}}$ = 0.002; Fig. 3E).

To measure how tilt responses developed, we recorded calcium signals from a transgenic line with sparse expression in superior oblique motor neurons (fig. S2). Motor neuron somata were stably positioned within nIV (Fig. 3, F to I), allowing reliable identification of the same neurons over 2-day increments: 3 to 5 dpf, 5 to 7 dpf, and 7 to 9 dpf. Almost every superior oblique neuron had a stronger response to 25° nose-up body tilts at 5 dpf than at 3 dpf ($P_{t\ \text{test}}$ = 1.31×10^{-16}, n = 59 pairs over N = 4 fish; Fig. 3J). Whereas the distributions of differences varied between 5 to 7 and 7 to 9 dpf ($P_{\text{K-S test}}$ = 5.7×10^{-15}; Fig. 3K), when evaluated across fish, the average response did not change between 5 to 7 dpf ($P_{t\ \text{test}}$ = 0.69, n = 53 cells/N = 4 fish) or 7 to 9 dpf ($P_{t\ \text{test}}$ = 0.23, n = 23/N = 3; Fig. 3L).

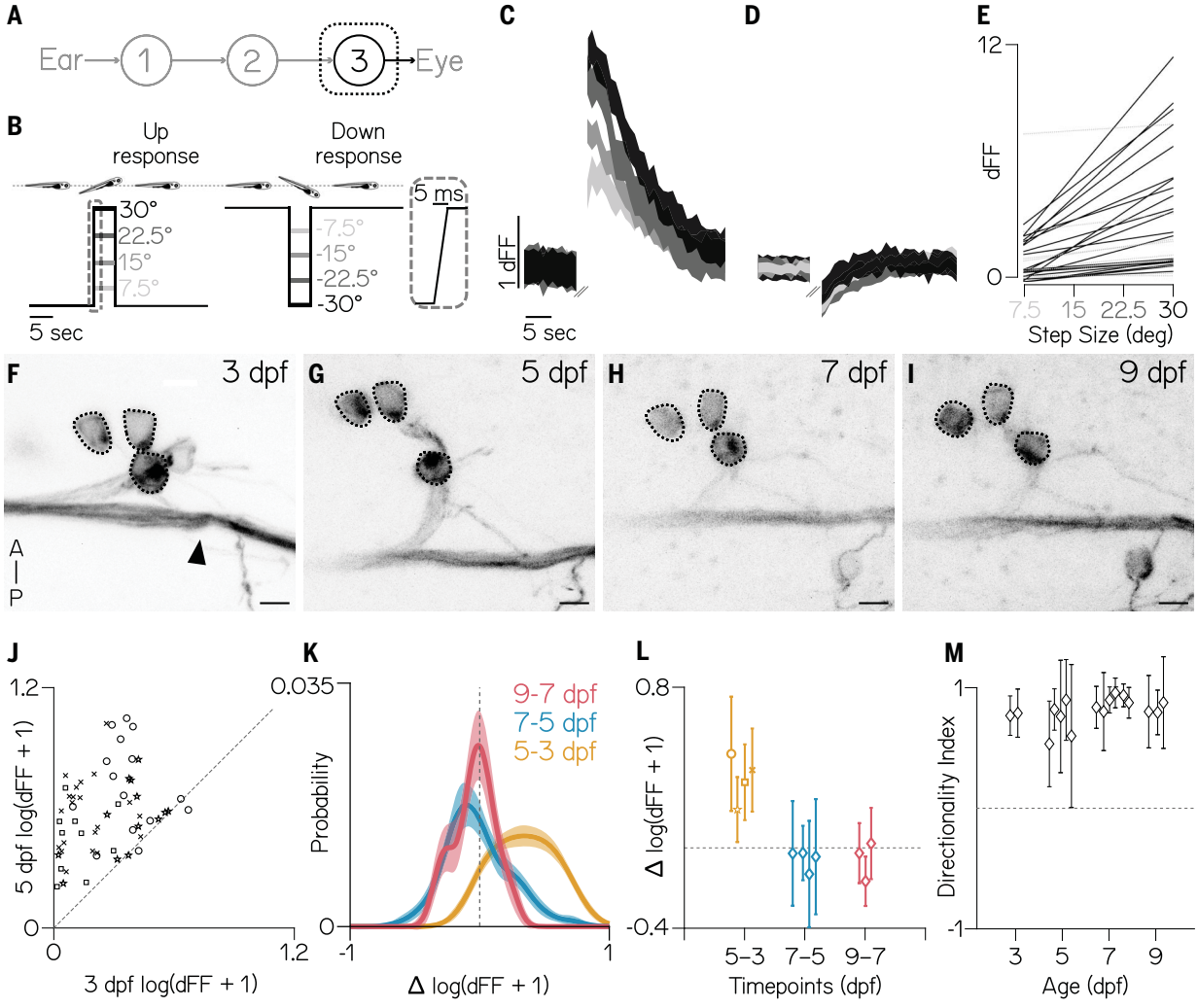

Fig. 3. Superior oblique motor neuron responses plateau between 3 and 5 dpf. (**A**) Diagram of the gaze stabilization circuit, focused on motor neurons. (**B**) A pitch-tilt stimulus trial with a 15-s baseline, a rapid step (inset, 30° step), a 5-s eccentric hold, and a rapid return for imaging. (**C** and **D**) Mean ± SD of responses (dFF) to nose-up (C) and nose-down (D) pitch steps from a single superior oblique extraocular motor neuron at 5 dpf (three to five trials per step size). Pitch amplitude (grayscale) as in (B). (**E**) Best-fit lines of responses (dFF) from superior oblique motor neurons to nose-up pitch tilts. Black lines have slopes > 0 (n = 22/32, N = 3 fish). (**F** to **I**) Three superior oblique extraocular motor neurons (dotted circles) and the trochlear nerve (black arrowhead) tracked from 3 to 9 dpf. Scale bars: 5 μm. A, anterior; P, posterior. (**J**) Comparison of neural responses (dFF) to 25° nose-up steps at 3 and 5 dpf ($P_{t\ \text{test}}$ = 1.31×10^{-16}). Dashed line at 0. (**K**) Distribution ± bootstrapped SD of pairwise differences of individual neurons between days (5 and 3, 7 and 5, and 9 and 7 dpf) in response to 25° nose-up steps. (**L**) Data from (K), plotted as the median pairwise difference for neurons from each individual fish (N = 4, 4, and 3). Five to 7 versus 7 to 9 dpf ($P_{t\ \text{test}}$ = 0.69 and 0.23, respectively). Dashed line at 0. (**M**) Median ± IQR directionality index to ±25° steps across ages ($P_{\text{K-W test}}$ = 0.09). +1 is selective for nose-up, −1 is selective for nose-down. Dashed line at 0.

We gathered another dataset with 19° nose-up and nose-down steps to evaluate the development of directional selectivity (see methods for details). We observed no changes across time ($P_{K\text{-}W\ test}$ = 0.09, 3 dpf: n = 16 neurons over N = 2 fish; 5 dpf: n = 32/N = 5; 7 dpf: n = 60/N = 7; 9 dpf: n = 30/N = 3; Fig. 3M). Brain activity related to the vestibulo-ocular reflex (*21*) must converge on extraocular motor neurons. Because extraocular motor neuron response strength and directional selectivity appear to plateau by 5 dpf—well before behavior—we conclude that the slowest component of the circuit to develop must lie downstream of motor neurons.

The developmental time course of the postsynaptic neuromuscular junction matches the maturation of behavior

We next focused on the extraocular neuromuscular junction (Fig. 4A). We labeled postsynaptic acetylcholine receptors with fluorescently conjugated alpha-bungarotoxin (α-BTX; Fig. 4, B to D) and presynaptic vesicles with an SV2A antibody (*22*) (Fig. 4, E to G). We targeted all four eye muscles used for torsional gaze stabilization: superior oblique (SO), superior rectus (SR), inferior oblique (IO), and inferior rectus (IR) in 3 to 9 and 14 dpf fish. Over time, the fraction of each muscle labeled with α-BTX increased with a time course comparable to behavioral improvement ($P_{ANOVA} < 10 \times 10^{-16}$) (SO, n = 106 muscles over N = 61 fish; SR, n = 52/N = 32; IR, n = 43/N = 28; IO, n = 38/N = 26; Fig. 4H), with no difference in labeling observed between 9 and 14 dpf ($P_{post\ hoc}$ = 0.185). In contrast, SV2A labeling appeared earlier and developed more rapidly. SV2A labeling significantly increased between 3 and 5 dpf ($P_{post\ hoc} = 5.5 \times 10^{-4}$) but did not change afterward ($P_{post\ hoc}$ > 0.13 for 5 to 7, 5 to 9, 5 to 14, 7 to 9, 7 to 14, and 9 to 14; SO, n = 34 cells/N = 17 fish; SR, n = 33/N = 17; IR, n = 29/N = 17; IO, n = 28/N = 15; Fig. 4I).

Larval zebrafish eye muscles assume their adult configuration by 3 dpf and develop both thick and thin myofibrils by 4 dpf (*23*), allowing the eye to assume static orientations up to ±30° (*14*) and a mature optokinetic response (<0.5 Hz) by 6 dpf (*24*). To evaluate whether eye velocity was constrained by the properties of the muscle, we measured eye movements at 5 dpf after unnaturally rapid tilts (90°/s, 600°/s^2 instead of 35°/s, 150°/s^2; fig. S3A). We found that although gaze stabilization behavior was far from mature, and the α-BTX signal had just begun to emerge, the eye could rotate faster ($P_{t\ test}$ = 0.016; fig. S3, B and C). Together, these findings implicate postsynaptic development at the neuromuscular junction as the slowest step in circuit maturation.

Vestibulo-ocular reflex behavior is mature after restoration of transient sensory deprivation

If sensory experience sets the rate of behavioral development, then transient loss of vestibular sensation should delay normal improvements to gaze stabilization. Upon restoration, vestibulo-ocular reflex performance should steadily improve. Alternatively, if behavioral performance reflects the capacity of the circuit component that matures most slowly, then upon restoration of vestibular sensation, behavior would be immediately comparable between experienced and transiently deprived larvae.

We investigated the emergence of the vestibulo-ocular reflex in a mutant line (*otogelin*) that, in

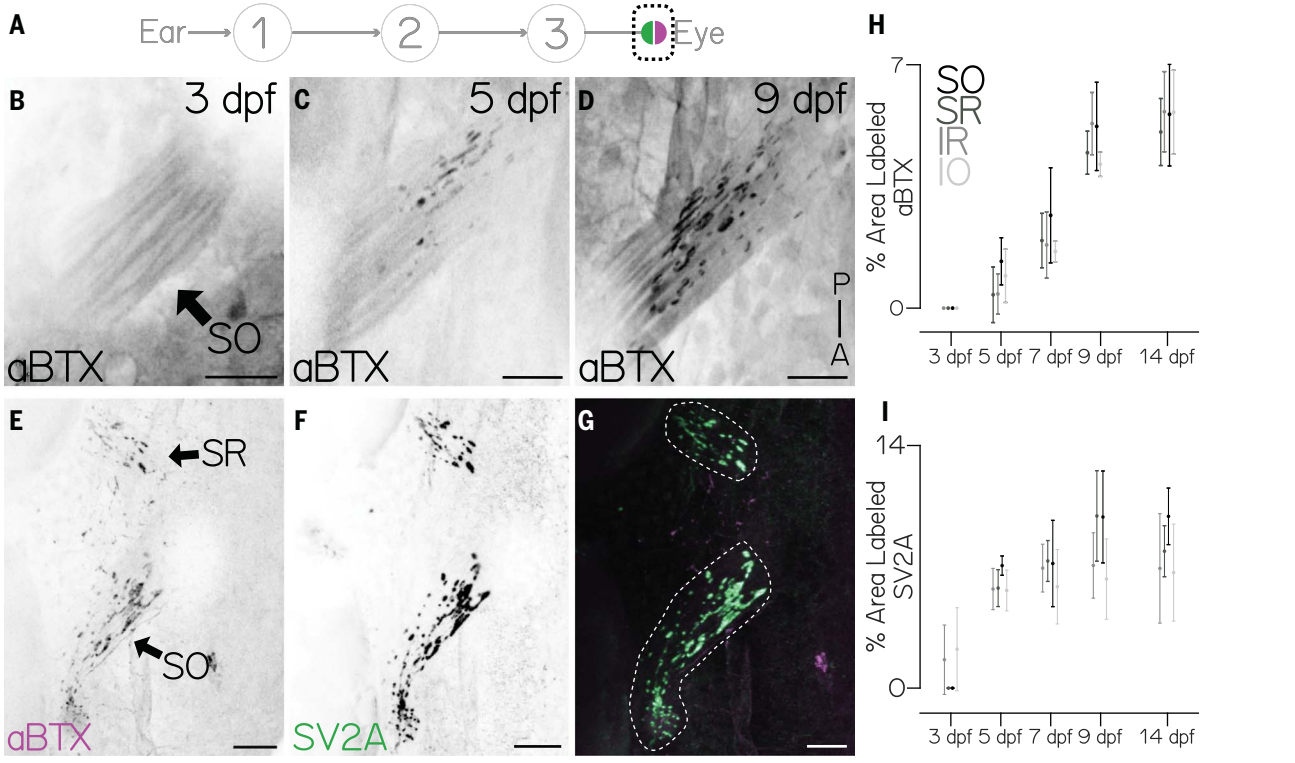

Fig. 4. The time course of postsynaptic neuromuscular junction development matches behavioral maturation. (**A**) Diagram of the gaze stabilization circuit, focusing on presynaptic (green) and postsynaptic (magenta) components of the neuromuscular junction. (**B** to **D**) Dorsal projection of the superior oblique muscle (black arrow) at 3 (B), 5 (C), and 9 (D) dpf labeled with fluorescent α-BTX. Scale bars: 20 μm. (**E** to **G**) Comparison of superior oblique (SO, arrow) and superior rectus (SR, arrow) presynaptic (SV2A, green) and postsynaptic (α-BTX, magenta) label at 8 dpf. Dashed line in (G) denotes muscle bound used for quantification. SO muscle: 6.59% α-BTX and 15.03% SV2A. SR muscle: 4.98% α- BTX and 9.33% SV2A. Scale bars: 20 μm. (**H**) Postsynaptic α-BTX label in SO, SR, inferior rectus (IR), and inferior oblique (IO) muscles. Dots are the mean ± SD area labeled. Three versus 9 dpf, $P_{ANOVA} < 10 \times 10^{-16}$; 9 versus 14 dpf, $P_{post\ hoc}$ = 0.185. (**I**) Presynaptic SV2A staining in SO, SR, IR, and IO. Dots are the mean ± SD area labeled. Three versus 5 dpf, $P_{post\ hoc} = 5.5 \times 10^{-4}$; 5 versus 7 dpf, $P_{post\ hoc}$ = 0.889; 7 versus 9 dpf, $P_{post\ hoc}$ = 0.462; 9 versus 14 dpf, $P_{post\ hoc}$ = 0.983.

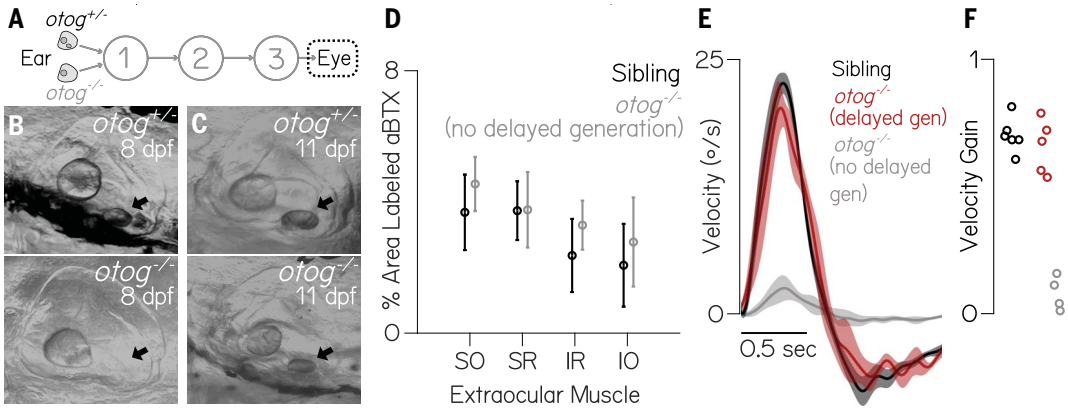

Fig. 5. Gaze stabilization behavior emerges rapidly after delayed emergence of tilt sensation. (**A**) Diagram of the gaze stabilization circuit illustrating *otogelin*$^{-/-}$ phenotype with focus on eye movements. (**B** and **C**) (Top) *otogelin*$^{+/-}$, utricular otolith visible in ear at 8 (left) and 11 dpf (right, black arrows). (Bottom) *otogelin*$^{-/-}$ fish without a utricular otolith at 8 dpf and with at 11 dpf (black arrows). (**D**) Postsynaptic α-BTX label from sibling and *otogelin*$^{-/-}$ fish in SO (N = 6 and 6), SR (N = 5 and 6), IR (N = 5 and 5), and IO (N = 4 and 6). (**E**) Average eye velocity traces ± SEM to a nose-up step as in Fig. 1B. (**F**) Vestibulo-ocular reflex gain (peak eye velocity divided by peak table velocity) for each fish (peak table velocity = 35°/s) (N = 6, 5, and 4) in (E). Gains in *otogelin*$^{-/-}$ fish with delayed utricular generation versus controls, $P_{post\ hoc}$ = 0.66; gains in *otogelin*$^{-/-}$ fish with no utricular generation versus controls, $P_{post\ hoc} = 1.84 \times 10^{-7}$; gains in *otogelin*$^{-/-}$ fish with no utricular generation versus *otogelin*$^{-/-}$ fish with delayed utricular generation, $P_{post\ hoc} = 6.20 \times 10^{-7}$.

some cases (*25*), is transiently insensitive to body tilts. Under normal conditions (*19*), larval zebrafish rely exclusively on the utricle to sense body tilts (*26*), which uses an inertial difference between an otolith and hair cells embedded in a gelatinous macula to transduce linear acceleration. Initial calcification of the utricular otolith normally occurs between 18 and 24 hours postfertilization (*27*). Most *otogelin* mutants do not generate a utricular otolith and as a result, in the dark, cannot sense body tilts (*28*). A small fraction of *otogelin* mutants show delayed generation of the utricular otolith, which appears over a 24-hour period at around 2 weeks of age (Fig. 5, B and C), at which point postural behaviors resume (*25*). We hypothesized that because the neuromuscular junction would have time to mature, *otogelin* mutants should show comparable behavior to siblings as soon as the utricle becomes functional.

We first confirmed that the neuromuscular junction developed normally in *otogelin* mutants; we observed strong α-BTX labeling at 8 dpf in both mutants and sibling controls in all four muscles (Fig. 5D). Next, we raised and screened >2000 *otogelin* mutants daily to identify five fish with nascent bilateral utricular otoliths between 11 and 16 dpf (see methods for details). Eye movements in response to body tilts were measured (Fig. 1B) on the day after identification, when the otolith had reached normal size. Performance was statistically indistinguishable between controls (N = 6) and mutants (N = 5) with newly generated otoliths ($P_{post\ hoc}$ = 0.66; Fig. 5, E and F). In contrast, 11 to 16 dpf fish that never developed otoliths were profoundly impaired ($P_{post\ hoc} = 1.84 \times 10^{-7}$ sibling versus no otolith, 6.20×10^{-7} delayed otolith versus no otolith). We infer from the rapid emergence of functional gaze stabilization in *otogelin* mutants that initial vestibular circuit assembly can proceed without sensory input, consistent with other reports (*25*, *29*, *30*). Our data show that vestibular experience is dispensable for maturation of the vestibulo-ocular reflex.

Discussion

We find that both the vestibulo-ocular reflex circuit and behavior can mature without any vestibular or visual input. This finding is particularly notable given that gaze stabilization is plastic later in life: Visual feedback from eye movements is used to adjust the sensitivity of central vestibular neurons to modulate gain (*5*). Even when there are no motor neurons to move the eyes, we see that central vestibular neuron responses to tilts are unchanged, underscoring the early dispensability of sensory feedback. In the light, the vestibulo-ocular and optokinetic reflexes work together to stabilize gaze; feedback from optokinetic eye movements might suffice to shape the vestibulo-ocular reflex circuit we studied here. However, such modulation would be inconsistent with our finding that the vestibulo-ocular reflex matures normally in congenitally blind fish. Studies of locomotor development over the past century underscore the importance of feedback as animals learn to move properly in their environment (*31*, *32*). Undoubtedly, given the considerable morphological and neurological changes that happen between larval and adult stages, feedback will be similarly important to maintain an excellent vestibulo-ocular reflex. We show that such plasticity acts on a mature scaffold that can evoke excellent behavior as soon as the neuromuscular junction is sufficiently developed.

By definition, evolutionary adaptations that support earlier or later development of sensorimotor reflex behaviors must manifest with changes at the circuit component that is slowest to develop—that is, a rate-limiting step. Does the rate of development of the neuromuscular junction limit maturation of other behaviors? Early neuromuscular junction development permits developing rodents to make spontaneous limb contractions, or "twitches," that can shape sensory cortical (*33*) and cerebellar development (*34*). Similar twitches (*35*) precede development of the hindbrain neurons responsible for evoked escape swimming in larval zebrafish (*36*), the earliest sensorimotor reflex behavior; by inference, the rate-limiting process for escapes is upstream of the motor periphery. Differences in the location of the rate-limiting process may reflect selective pressures that differ between precocial (mobile at birth) and altricial (immobile) animals. Empirically, when the pressure is on to stand (or run or swim) or be eaten, the motor periphery develops much more rapidly to ensure that "the neuromuscular system [is] ready for use when the brain needs it" (*37*). We suggest that defining the location of rate-limiting processes will provide critical insights into how brain circuits develop.

Recent advances in transcriptomics and connectomics (*7*, *8*) revealed the elements of and interactions between vertebrate neural circuit nodes. Similar advances transformed longitudinal (*38*) and circuit-level (*39*) measurements linking neuronal activity and behavior (*40*). In contrast, conceptual frameworks (*41*) lag behind, relying primarily on classic loss-of-function approaches to establish necessity (*42*). Here, we propose a candidate rate-limiting process for the maturation of a vertebrate sensorimotor behavior. Our approach moves beyond "necessity" (*43*), linking neural circuit development to behavioral performance.

REFERENCES AND NOTES

1. D. H. Hubel, T. N. Wiesel, *Naunyn Schmiedebergs Arch. Pharmakol.* **248**, 492–497 (1964).
2. E. F. Chang, M. M. Merzenich, *Science* **300**, 498–502 (2003).
3. M. Jamon, *Front. Integr. Neurosci.* **8**, 11 (2014).

4. C. T. Goode, D. L. Maney, E. W. Rubel, A. F. Fuchs, *J. Neurophysiol.* **85**, 1119–1128 (2001).
5. S. du Lac, J. L. Raymond, T. J. Sejnowski, S. G. Lisberger, *Annu. Rev. Neurosci.* **18**, 409–441 (1995).
6. F. F. Blackman, *Ann. Bot.* **os-19**, 281–296 (1905).
7. J. Zhou *et al*., *Nature* **624**, 355–365 (2023).
8. L. Yuan, X. Chen, H. Zhan, G. L. Henry, A. M. Zador, *Nat. Commun.* **15**, 8371 (2024).
9. M. E. Thomason, *Biol. Psychiatry* **88**, 40–50 (2020).
10. H. Straka, R. Baker, *Front. Neural Circuits* **7**, 182 (2013).
11. J. M. Goldberg *et al*., *The Vestibular System: A Sixth Sense* (Oxford Univ. Press, 2012).
12. J. Szentágothai, *J. Neurophysiol.* **13**, 395–407 (1950).
13. M. Beraneck, F. M. Lambert, S. G. Sadeghi, in *Development of Auditory and Vestibular Systems*, R. Romand, I. Varela-Nieto, Eds. (Elsevier, ed. 4, 2014), pp. 449–487.
14. I. H. Bianco *et al*., *Curr. Biol.* **22**, 1285–1295 (2012).
15. Y. Zhu *et al*., *Cell Rep.* **42**, 112573 (2023).
16. K. R. Hamling, Y. Zhu, F. Auer, D. Schoppik, *J. Neurosci.* **43**, 936–948 (2023).
17. T.-W. Chen *et al*., *Nature* **499**, 295–300 (2013).
18. D. Schoppik *et al*., *J. Neurosci.* **37**, 11353–11365 (2017).
19. D. Goldblatt *et al*., *Curr. Biol.* **33**, 1265–1281.e7 (2023).
20. D. Goldblatt *et al*., *eLife* **13**, RP96893 (2024).
21. G. Migault, N. Beiza-Canelo, S. Chatterjee, G. Debrégeas, V. Bormuth, bioRxiv 2024.03.22.586054 [Preprint] (2024); https://doi.org/10.1101/2024.03.22.586054.
22. K. Buckley, R. B. Kelly, *J. Cell Biol.* **100**, 1284–1294 (1985).
23. S. S. Easter Jr., G. N. Nicola, *Dev. Psychobiol.* **31**, 267–276 (1997).
24. J. C. Beck, E. Gilland, D. W. Tank, R. Baker, *J. Neurophysiol.* **92**, 3546–3561 (2004).
25. R. Roberts, J. Elsner, M. W. Bagnall, *J. Assoc. Res. Otolaryngol.* **18**, 415–425 (2017).
26. B. B. Riley, S. J. Moorman, *J. Neurobiol.* **43**, 329–337 (2000).
27. B. B. Riley, C. Zhu, C. Janetopoulos, K. J. Aufderheide, *Dev. Biol.* **191**, 191–201 (1997).
28. T. T. Whitfield *et al*., *Development* **123**, 241–254 (1996).
29. F. Ulrich, C. Grove, J. Torres-Vázquez, R. Baker, *Curr. Neurobiol.* **7**, 62–73 (2016).
30. D. L. Barabási, G. F. P. Schuhknecht, F. Engert, *Nat. Commun.* **15**, 364 (2024).
31. K. E. Adolph, B. I. Bertenthal, S. M. Boker, E. C. Goldfield, E. J. Gibson, *Monogr. Soc. Res. Child Dev.* **62**, i–162 (1997).
32. E. Thelen, *Int. J. Behav. Dev.* **24**, 385–397 (2000).
33. R. Khazipov *et al*., *Nature* **432**, 758–761 (2004).
34. J. C. Dooley, G. Sokoloff, M. S. Blumberg, *Curr. Biol.* **31**, 5501–5511.e5 (2021).
35. L. Saint-Amant, P. Drapeau, *J. Neurobiol.* **37**, 622–632 (1998).
36. R. C. Eaton, R. D. Farley, *Copeia* **1973**, 673–682 (1973).
37. D. Kernell, *Neurosci. Biobehav. Rev.* **22**, 479–484 (1998).
38. N. A. Steinmetz *et al*., *Science* **372**, eabf4588 (2021).
39. T. Nöbauer, Y. Zhang, H. Kim, A. Vaziri, *Nat. Methods* **20**, 600–609 (2023).
40. S. Schneider, J. H. Lee, M. W. Mathis, *Nature* **617**, 360–368 (2023).
41. D. L. Barabási *et al*., *J. Neurosci.* **43**, 5989–5995 (2023).
42. Y. Lazebnik, *Cancer Cell* **2**, 179–182 (2002).
43. S. Brenner, *Curr. Biol.* **5**, 332 (1995).
44. D. Schoppik, Data associated with "Sensation is Dispensable for the Maturation of the Vestibulo-ocular Reflex," Open Science Foundation (2024); https://doi.org/10.17605/OSF.IO/7Z5UP.

ACKNOWLEDGMENTS

We thank C. Moens and M. Bagnall for all the fish; H. Gelnaw for assistance with husbandry; and K. Nagel, J. Dasen, N. Ringstad, L. Kiorpes, M. Long, G. Buzsáki, A. Schier, C. Desplan, S. Burden, and members of the Schoppik and Nagel labs for their valuable feedback and discussions. **Funding:** National Institute on Deafness and Communication Disorders of the National Institutes of Health award number R01DC017489 (D.S.); National Institute on Deafness and Communication Disorders of the National Institutes of Health award number F31DC020910 (P.L.); National Institute for Neurological Disorders and Stroke of the National Institutes of Health award number F99NS129179 (D.G.); National Science Foundation under Graduate Research Fellowship number DGE2041775 (P.L.). **Author contributions:** Conceptualization: P.L. and D.S. Data curation: P.L. Formal analysis: P.L. Funding acquisition: P.L., D.G., and D.S. Investigation: P.L., C.B., and C.Q. Methodology: P.L. and D.S. Project administration: D.S. Resources: B.R. and D.G. Software: P.L. and D.S. Supervision: P.L. and D.S. Validation: C.B. Visualization: P.L. and D.S. Writing – original draft: P.L. Writing – review & editing: P.L. and D.S. **Competing interests:** The authors declare that they have no competing interests. **Data and materials availability:** All raw data and analysis code are available at the Open Science Foundation (*44*).

SUPPLEMENTARY MATERIALS

science.org/doi/10.1126/science.adr9982
Materials and Methods
Figs. S1 to S3
References (*45*–*59*)
MDAR Reproducibility Checklist

Submitted 24 July 2024; accepted 6 November 2024
10.1126/science.adr9982